Surface Area Increase of Silicon Alloys in Li-Ion Full Cells Measured by Isothermal Heat Flow Calorimetry

L. J. Krause,[*,z] **T. Brandt, V. L. Chevrier,**[*] **and L. D. Jensen**

Corporate Research Materials Laboratory, 3M Center, St. Paul, Minnesota 55144-1000, USA

Li-ion pouch cells utilizing a negative electrode formulated with 15 wt% of an engineered Si alloy in a graphite composite electrode were cycled in an isothermal heat flow calorimeter against a $LiCoO_2$ positive electrode. Two different electrolytes were investigated: a blend of ethylene carbonate and ethyl methyl carbonate (3EC:7EMC) and a blend of ethylene carbonate, ethyl methyl carbonate and 1-fluoro ethylene carbonate (27EC:63EMC:10FEC). Both electrolytes were 1 M in $LiPF_6$ salt. The parasitic thermal power and coulombic efficiency was derived from isothermal heat flow measurements and high precision current-source meters. Cells without FEC showed high parasitic thermal power which increased with cycle number indicative of a surface area increase which was confirmed by post-cycling scanning electron micrographs and surface area measurements. Cells with FEC showed relatively stable parasitic thermal power. These measurements demonstrate the surprising function of FEC in controlling or attenuating the evolution of surface area in Si alloys. Vinylene carbonate was also found to be effective at controlling the increase in alloy surface area.

Meeting the promise of silicon or Si alloys to increase the energy density of Li-Ion cells has been the subject of a great deal of research and development. To date the full commercial impact of this materials technology has not been met owing to the difficulties found with silicon.[1–6] In general the high capacity fade often found in Li-ion cells containing Si has 3 main causes: 1) mechanical or electrical disconnect of the alloy particles in the composite electrode owing to large volume changes[1–4] 2) crystallization effects, mainly the formation of the $Li_{15}Si_4$ phase, which shows high irreversibility[5–7] and 3) unusual electrolyte reactivity.[3,6,8,9] It is the latter failure mechanism which this paper addresses.

It has been recognized and shown by many that the electrolyte composition can be crucial for cycling capacity in cells containing silicon or Si alloys.[9,10] Recent work by Petibon et al. on pouch cells using a negative electrode composed of 72.3 wt% graphite, 15 wt% Si alloy, 10 wt% KS6 and 2.7 wt% carboxymethyl cellulose-butadiene styrene binder (CMC:SBR) showed approximately 300 cycles to 80% of the original capacity at a C/2 rate. In that work the base electrolyte was 1 M $LiPF_6$ in a blend of EC, EMC and FEC in the weight ratios of 27:63:10 respectively. The capacity fade was linear until about 250 cycles at which point the capacity fade rate accelerated significantly.[4] The authors showed that the additive FEC was consumed during cycling and the acceleration of the fade rate occurred when the FEC was consumed. Analysis of the gas produced during the first cycle was shown to be mainly CO_2 with small amounts of H_2 and CO. The authors attributed the gas formed as products from the reductive formation of SEI layers at the graphite and alloy surfaces. They argued that the absence of ethylene suggests that FEC inhibits the reduction of EC and noted DFT calculations by Leung et al. suggesting that FEC can undergo a 1-electron reduction at the Si surface to form CO_2 and LiF among other products.[11] As Petibon et al. noted, the reaction pathways for the reduction of FEC are not clear and others have suggested alternative reaction pathways that do not produce gas.[4]

Others have also investigated the effect of FEC on the cycling characteristics of Si electrodes. Studies by the Lucht group have shown a dramatic difference in the capacity retention of Si electrodes with and without the addition of FEC.[9,10] They suggested that polymeric species associated with the reduction of FEC and VC are deposited on the Si surface providing passivation.[10] Many authors have seen an increase in the abundance of LiF as a component of the SEI formed on the Si electrode.[3,11] In the absence of FEC, Nakai et al. found evidence that Si is eroded during cycling yielding higher abundances

of Silicon-oxygen containing species.[8] Choi et al. have suggested that the interface between the Si and the electrolyte contains EC reduction intermediates that are less dense than the derivatives formed when the electrolyte contains FEC and electrolyte decomposition can continue in the absence of FEC.[12]

In this paper we compare the parasitic thermal power, obtained by isothermal heat flow calorimetry, of 230 mAh full cell pouch cells containing an engineered Si alloy as a component of the negative electrode. We show that cells without FEC as an additive develop very large parasitic thermal power as a function of cycle number consistent with an increase in surface area. Cross sectional microscopy and BET surface area measurements of cycled electrodes support this conclusion. Cells containing FEC do not develop high surface area and the parasitic thermal power remains relatively constant as a function of cycle number. To our knowledge this increase in surface area, unique to the electrolyte formulation, has not been previously recognized

Experimental

Machine wound pouch cells were used in this work. They were obtained from LiFUN Technology (Xinma Industry Zone, Hunan Province, China) as sealed dry cells with a nominal capacity of 230 mAh. The composition of the negative electrode was 15 wt% Si alloy, 70.7 wt% artificial graphite (BTR-918), 0.3 wt% Super P (Imerys), 4 wt% KS6 (Imerys) and 10 wt% of a water soluble binder based on lithium polyacrylate. The latter is the primary difference from Petibon et al. in electrode formulation. The alloy is identical to that used by Petibon et al., with a reversible capacity of 1180 mAh/g, a density of 3.5 g/cm^3, a surface area of 6.9 m^2/g and a median particle size of 5.2 μm. The positive electrode was $LiCoO_2$. The cells were balanced to a 4.35 V charge voltage. The first cycle reversible areal capacity was 2.45 mAh/cm^2. Table I shows the general electrode parameters.

Table I. Full cell information.

Parameter	Anode	Cathode
Formulation	70.7% BTR-918/15% Si alloy/4% KS6/0.3% SP/10% binder	97% HVLCO
Coating weight (mg/cm^2)	8.5	20.8
Nominal porosity (%)	30%	20%
Collector	Copper	Aluminum
Collector thickness (μm)	15	20

*Electrochemical Society Member.

[z]E-mail: ljkrause@mmm.com

The cells were first opened in a dry room and dried at 70°C under vacuum overnight. The cells were then filled with 0.9 g of electrolyte in a dry room with an operating dew point of −50°C. The cell filling procedure employed brief, periodic vacuum degassing in order to allow the electrolyte to access all void volume within the cell's electrodes. The weight before and after the electrolyte filling procedure was recorded in order to ensure the weight of electrolyte added to each cell was consistent. The pouch cells were then sealed under vacuum in a MSK-115A vacuum sealing machine (MTI Corp.) The cells were allowed to stand for 24 hours prior to cycling to ensure complete wetting, no charge was applied during standing.

The base electrolyte used in this work was 1 M LiPF$_6$ in a 3/7 (w/w) blend of ethylene carbonate (EC) and ethyl methyl carbonate (EMC) obtained from BASF and used as received. VC (Novolyte) and FEC (BASF) were also used as received. All solvents, salts and blends were stored in a dry box located within a dry room.

Current source.—Keithley 2602A source-measure units were used to charge and discharge the cells. This equipment is capable of supplying currents in the 10 mA to 100 mA range with an accuracy of ± 0.03% + 6 μA with a resolution of 200 nA. The voltage measurement accuracy is ± 0.015% + 1 mV with 10 μV resolution in the 6 V range. Time resolution is < 1 sec. This precision allows the measurement of the coulombic efficiency to within ±0.02%.

Isothermal heat flow calorimeter.—The heat flow calorimeter is a TAM III (Thermally Activated Module, TA Instruments) in which 12 calorimeters were inserted. The temperature used throughout this work was 37°C. The TAM III is capable of controlling the bath temperature to within a few micro-degrees centigrade. Reference 13 describes the method and modifications made to the TAM III to allow in-operando calorimetry measurements on Li-ion cells. Further details for adapting the TAM III calorimeter to parasitic measurements with pouch cells can be found in Reference 14.

Cycling protocol.—The protocol for cycling cells in the isothermal heat flow calorimeter was as follows: cells were cycled 10 times in each of the voltage segments of 3.0–3.8, 3.5–3.8, 3.7–3.9, 3.8–4.0, 3.9–4.1 and 4.0–4.25 V. The current for all cycles was 20 mA, nominally C/11 for a full voltage range of 3.0–4.25 V. Ten cycles per voltage segment resulted in a nominally stable coulombic efficiency and average parasitic thermal power for a given voltage segment as described in an earlier publication.[14] The last cycle of each voltage segment was then used to construct a plot of parasitic thermal power versus the average voltage of the segment. We note that in the method we use here, coulombic efficiency, or inefficiency, is simultaneously collected with the thermal data for each voltage segment.

We have reported on this cycling protocol previously in a study of electrolyte chemistry of graphite//LiCoO$_2$ cells.[13] In the present work, where two materials with distinctly different voltage versus capacity characteristics are considered (i.e. Si and graphite), the lithiation and delithiation does not occur uniformly for both materials under all voltage segments. This is discussed below.

Methods.—The treatment of data to arrive at a parasitic thermal power by this method has been described in detail earlier.[13,14] This method, termed the "integration/subtraction" method, yields an average parasitic thermal power at a given average voltage. Briefly, a total thermal energy is first obtained from the calorimetry data over one cycle. Secondly, the energy loss over one cycle is calculated using the voltage and current (corresponds to the hysteresis area in a voltage-capacity plot). Subtracting the energy loss from the total thermal energy yields a parasitic energy. Dividing the parasitic energy by the cycle time yields an average parasitic thermal power, which can be compared across cycles of various durations.

Cross section and surface area.—In a dry room, cycled electrodes were rinsed in DMC and ion beam polished cross section were obtained with a JEOL IB-09010CP Cross Section Polisher. Cross sec-
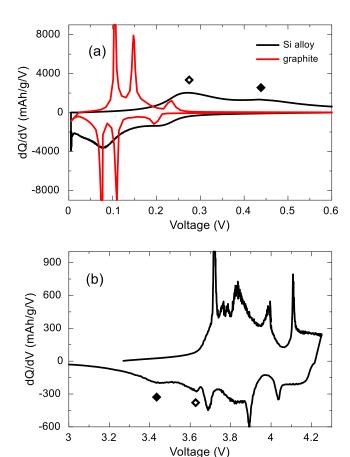

Figure 1. (a) Differential capacity (dQ/dV vs V) curves of Si alloy and graphite half cells, Si alloy delithiation peaks are identified by diamonds. (b) Differential capacity curve of a Gr:Si-alloy//LCO full cell with the corresponding Si alloy delithiation peaks marked by diamonds.

tion imaging was performed with a Hitachi s-4700 Field Emission Scanning Electron Microscope (FESEM).

BET surface area measurements were performed with a Quantachrome Nova 4000e. The cells were held at 1.5 V for 100 hours to attempt to fully delithiate the negative electrode. The cells were then opened in a dry room and the negative electrode unwound from the jelly roll. The electrode was then immersed in dimethyl carbonate for one to two hours to remove electrolyte and salt. The electrode material was then scraped from the Cu current collector by a razor and the powder dried under vacuum.

Results

Effect of cycling protocol.—The voltage segments used in this work will have different effects on graphite and silicon due to their distinct voltage curves. For example, in higher full cell voltage ranges the Si alloy may be fully lithiated but is not cycled. Figure 1a shows plots of dQ/dV vs V for a Si alloy/binder half cell and a graphite half cell. Figure 1a shows that for the Si component, full delithiation will only occur if the discharge voltage is above 0.5 V vs Li. Figure 1b shows a plot of dQ/dV vs V for the full cell pouch cells used in this work. Highlighted in Figure 1b are the peaks associated with Si alloy delithiation. Under the cycling protocol used here, voltage segments with a discharge voltage above 3.8 V result in only the graphite component of the electrode undergoing lithiation and delithiation, as the Si alloy remains in a lithiated state. Therefore, under voltage segments with a lower voltage cutoff of 3.8 V and above, the thermal parasitics, and to a large extent the CIE, will be reflective of the graphite component of the electrode and dormant lithiated Si alloy.
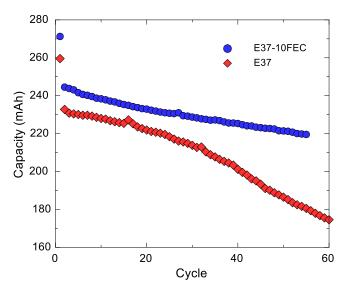
Figure 2. Cycle life of Gr:Si-alloy//LCO full pouch cells with 3EC:7EMC or 23EC:67EMC:10FEC in 1 M LiPF$_6$ as indicated by the legend.

Figure 3. (a) Parasitic power and (b) coulombic inefficiency of Gr:Si-alloy//LCO full pouch cells with 3EC:7EMC in 1 M LiPF$_6$ electrolyte as a function of the average voltage window for various cycle numbers as indicated in the legend.

Figure 2 shows typical results from constant current cycling of Si alloy containing cells between 3.0 and 4.25 V at room temperature. The normalized capacity versus cycle results are for Gr:Si-alloy//LCO cells with an electrolyte blend of 27EC:63EMC:10FEC and an electrolyte blend of 3EC:7EMC, both with 1M LiPF$_6$. It is clear that the cell without FEC has a much greater fade rate, consistent with previously published results.[1,4]

Thermal parasitics and coulombic efficiency.—Parasitic thermal power and coulombic efficiencies of Gr:Si-alloy//LCO cells were studied as a function of cycle number and electrolyte composition using two groups of cells. One group was filled with an electrolyte blend of 3EC:7EMC and the other group was filled with a blend of 27EC:63EMC:10FEC. Cells were cycled between 3.0 and 4.25 V at room temperature under constant current conditions at a nominal C/8 rate (30 mA). After a given number of cycles ranging from 10 to 75, cells were stopped and inserted into the isothermal micro-calorimeter at 37°C. Figures 3a and 3b show the parasitic thermal power and coulombic inefficiency respectively of cells without FEC. Figure 3a shows the parasitic thermal power increases dramatically from a cell with 10 cycles to one with 75 cycles. Figure 3b shows the coulombic inefficiency increases dramatically also, correlating with the thermal power shown in Figure 3a. Note that the cells with 60 and 75 cycles show a decrease in both parasitic thermal power and CIE at the highest voltage segment (4.0–4.25 V) where the Si alloy is highly lithiated but not cycling.

Figures 4a and 4b show the corresponding parasitic thermal power and CIE for the group of cells with 10 wt% FEC. The parasitic thermal power of this group of cells with 10% FEC is far lower than the cells without the FEC additive over the entire cycle life protocol. The CIE also remains relatively constant with cycle number. Figures 5a and 5b show the parasitic thermal power at 3.8 V and CIE of both sets of cells plotted on the same axis to highlight how dramatic the differences are in the magnitude and relative stability of the group of cell with and without 10% FEC.

The parasitic thermal power extracted in these measurements is the result of reaction enthalpies of the various irreversible electrode/electrolyte reactions occurring in the cell and the kinetics of these reactions. As long as these processes remain constant no change in the parasitic thermal power as a function of cycle number would be expected. In an earlier work we showed how graphite//LCO cells cycled under similar conditions in the heat flow calorimeter maintained a near constant thermal power over many cycles.[14] Clearly the Gr:Si-alloy//LCO cells without FEC measured here do not conform to this
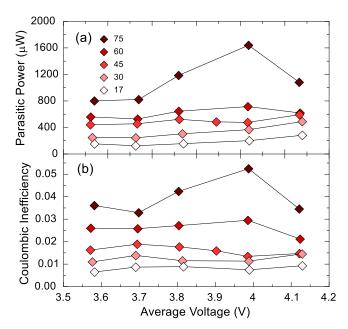
expected stability. The increase in CIE associated with the increase in thermal power shows that the massive change in thermal power cannot be due to a dramatic change in reaction enthalpy and therefore the increase in thermal power must be due to an increase in the molar rate of reaction per cycle. This can occur if there is a change in active surface area. We showed previously that higher initial surface areas result in higher thermal power and higher CIE.[13] Furthermore, high precision coulometry experiments have also shown the dependence of coulombic efficiency and active surface area.[13]
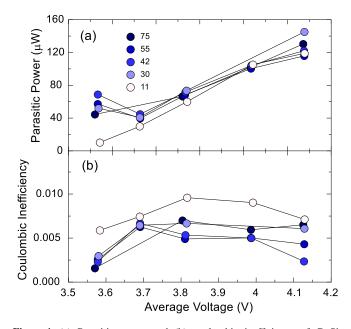

Figure 4. (a) Parasitic power and (b) coulombic inefficiency of Gr:Si-alloy//LCO full pouch cells with 23EC:67EMC:10FEC in 1 M LiPF$_6$ electrolyte as a function of the average voltage window for various cycle numbers as indicated in the legend.
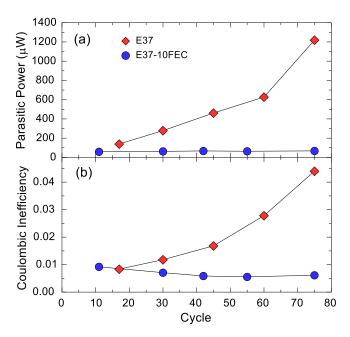
Figure 5. (a) Parasitic power and (b) coulombic inefficiency for Gr:Si-alloy//LCO full pouch cells with 3EC:7EMC or 23EC:67EMC:10FEC in 1 M LiPF$_6$ as indicated by the legend. Values were interpolated from Figures 3 and 4 at an average voltage of 3.8 V.

Figure 7. FESEM cross section images of negative electrodes from Gr:Si-alloy//LCO full pouch cells with 3EC:7EMC or 23EC:67EMC:10FEC in 1 M LiPF$_6$. (a) Without FEC after 30 cycles, (b) with FEC after 30 cycles, (c) without FEC after 75 cycles, and (d) with FEC after 75 cycles.

Electrode cross sections.—To confirm this interpretation the negative electrodes from both sets of electrolyte groups were cross sectioned and imaged. Figures 6a through 6d show the morphology change of the Si alloy containing negative electrodes without any cycling (fresh) and after 30, 45 and 60 cycles without FEC. The fresh electrode shows sharp, bright particles of Si alloy. Cycling results in the formation of a gray material covering the particle, which thickens with cycle number. The Si alloy particles also become perforated with the gray material and develop "hair like" structures at higher cycle numbers (Figure 6d). Figure 6 is consistent with an increasing surface area and thickness of SEI layer. Figures 7a through 7d compare the electrode cross sectional images of electrodes cycled with 10 wt% FEC with those cycled in the base electrolyte without FEC at two different cycle numbers. In Figures 7a and 7b the difference is not especially dramatic, but the cells have been cycled only 30 times. The
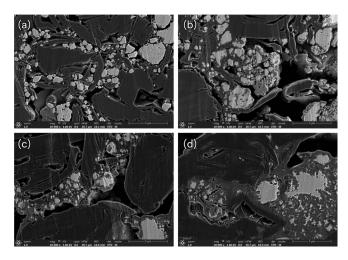
heat flow and CIE without FEC (Figures 5a and 5b) start to increase significantly beyond 30 cycles. Figures 7c and 7d show particle morphology after 75 cycles. Now the particle morphology has become distinctly different and shows significant erosion of the alloy particles in the cells without FEC. Also the maximum difference in parasitic thermal power and CIE are found between cells with and without FEC after 75 cycles. The cross-sectional analysis confirms a significant erosion of alloy particles occurring in cells without FEC but also shows that within the formed SEI there must be active particles or sites that can still undergo irreversible electrolyte reactions in order to sustain such high parasitic thermal power.

We also attempted BET surface area measurements on the cycled electrodes. To prepare and condition the electrodes for this measurement the full cells were discharged to 1.5 V and held for 100 hours. This was done in order to fully delithiate the negative electrode since they would be exposed to regular air for this analysis. Figure 8 shows the BET surface area of the cycled electrodes. Figure 8 shows the surface area of the cells cycled without FEC increases with cycle

Figure 6. FESEM cross section images of negative electrodes from Gr:Si-alloy//LCO full pouch cells with 3EC:7EMC in 1 M LiPF$_6$. (a) Fresh electrodes, (b) after 30 cycles, (c) after 45 cycles, and (d) after 60 cycles. Light and dark gray areas correspond to Si alloy and graphite, respectively.
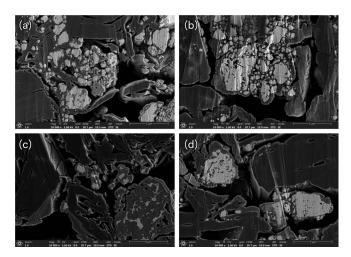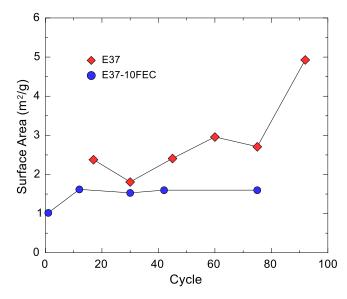

Figure 8. BET surface area of negative electrodes from Gr:Si-alloy//LCO full pouch cells with 3EC:7EMC (red diamonds) or 23EC:67EMC:10FEC (blue circles) in 1 M LiPF$_6$, as a function of cycle number.
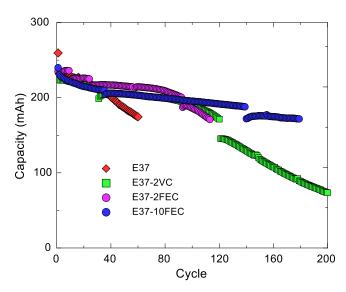
Figure 9. Cycle life of Gr:Si-alloy//LCO full pouch cells with 3EC:7EMC and additives as indicated in the legend.

Figure 10. (a) Parasitic power and (b) coulombic inefficiency of Gr:Si-alloy//LCO full pouch cells with 3EC:7EMC and 2 wt% FEC or 10 wt% FEC in 1 M LiPF$_6$ as a function of the average voltage window for various cycle numbers as indicated in the legend.

number while the surface area of the cells cycled with 10 wt% FEC remains essentially constant over the number of cycles investigated. These results are in qualitative agreement with the heat flow and CIE data as well as the cross sectional images. Only qualitative agreement is claimed as it is difficult to estimate the error on this measurement. Li reaction products with ambient air resulting from active materials that were not fully delithiated or any leftover electrolyte salt could impact this measurement. Indeed the electrochemical surface area and its increase is best and most reliably measured by the isothermal heat flow calorimeter coupled with the CIE measurement whereas the BET surface area, even if highly reliable, would not necessarily represent the electrochemical surface area. Parasitic heat flow as a measure of surface area for Si-based materials assumes an unchanging reaction enthalpy, which previous studies support.[15] The correlation between parasitics and initial surface area for active materials has been known for many years, however this is the first time, to our knowledge, that an increase in surface area with cycle number has been measured and correlated with increasing parasitics.

Low concentrations of FEC and VC.—As noted above, Petibon et al. saw a rather sudden change in fade rate at approximately 300 cycles under high rate cycling conditions (C/2). These authors used the same electrolyte formulation with 10 wt% FEC as used in the present work and the sudden failure was associated with the complete consumption of FEC.[4] In the present work we did not observe sudden failure using an electrolyte formulation with 10 wt% FEC. This is likely due to our use of a much slower cycling rate and insufficient cycle count. However sudden failure was observed using an electrolyte formulation with either 2 wt% FEC or 2 wt% VC. Figure 9 shows the cycle life of Gr:Si-alloy//LCO full cells with 2 wt% VC, 2 wt% FEC and 10 wt% FEC in 1 M LiPF$_6$ 3EC:7EMC. Figure 9 shows the cells with 2 wt% VC or FEC undergo a significant change in fade rate at approximately 90 cycles while the fade rate of the cell with 10 wt% FEC remains constant. Figure 10a shows the parasitic thermal power of the cells with 2 wt% FEC at cycle 10 and cycle 110 as well as for the cell with 10 wt% FEC at cycle 140. The parasitic thermal powers at cycle 10 with 2 wt% FEC are nearly identical to those at cycle 140 for the cell with 10 wt% FEC. However, the parasitic thermal power at cycle 110 with 2 wt% FEC increase dramatically. The rise in parasitic power is consistent with the rapid capacity fade and implied complete consumption of FEC. These results provide a phenomenological view into the failure that occurs with complete FEC consumption. Once the FEC is consumed, the behavior of the cell becomes similar to that of a cell without FEC. Indeed, increased
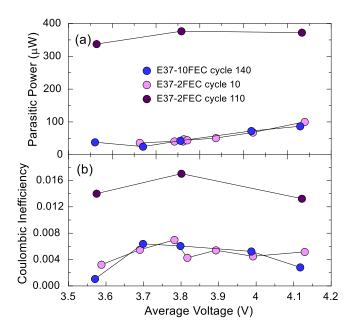
electrolyte reactivity and surface area lead to lithium consumption and rapid fade. Similar results were found for the use of VC as an additive. Figures 11a and 11b show the parasitic thermal power and CIE versus the average segment voltage for cells with 2 wt% VC. Here again near the inflection point for the onset of sudden failure the parasitics and CIE rise significantly as the surface area presumably begins to increase. This suggest that the passivation provided by FEC, while much improved over the base electrolyte, is not providing optimal passivation of the alloy surface and the repeated volume expansion
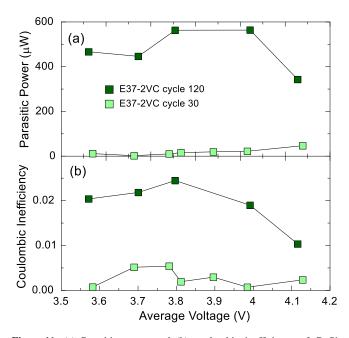

Figure 11. (a) Parasitic power and (b) coulombic inefficiency of Gr:Si-alloy//LCO full pouch cells with 3EC:7EMC and 2 wt% VC in 1 M LiPF$_6$ as a function of the average voltage window for 30 and 120 cycles as indicated in the legend.

and contraction leads to the exposure of fresh non-passivated surfaces which continually drive the additive consumption.

Summary

The electrolyte induced cycle life failure of Gr:Si-alloy//LiCoO$_2$ cells was shown by calorimetric and precision cycling methods to be an expansion of effective surface area where the formed SEI likely contains active electrochemical surfaces. FEC, used ubiquitously as an additive to improve the cycle life of Si-containing cells was shown to greatly attenuate the surface area expansion most likely through the formation of a denser and more resilient SEI. Sudden capacity failure, observed after FEC has been consumed was also shown to be accompanied by surface area expansion.

References

1. M. N. Obrovac and V. L. Chevrier, "Alloy negative electrodes for Li-ion batteries," *Chem. Rev.*, **114**, 11444 (2014).
2. M. N. Obrovac, L. Christensen, D. B. Le, and J. R. Dahn, "Alloy Design for Lithium-Ion Battery Anodes," *J. Electrochem. Soc.*, **154**, A849 (2007).
3. K. Schroder et al., "The Effect of Fluoroethylene Carbonate as an Additive on the Solid Electrolyte Interphase on Silicon Lithium-Ion Electrodes," *Chem. Mater.*, **27**, 5531 (2015).
4. R. Petibon et al., "Studies of the Capacity Fade Mechanisms of LiCoO$_2$/Si-Alloy: Graphite Cells," *J. Electrochem. Soc.*, **163**, A1146 (2016).
5. R. Petibon et al., "Studies of the Capacity Fade Mechanisms of LiCoO$_2$/Si-Alloy: Graphite Cells," *J. Electrochem. Soc.*, **163**, A1146 (2016).
6. D. J. Xiong et al., "Studies of Gas Generation, Gas Consumption and Impedance Growth in Li-Ion Cells with Carbonate or Fluorinated Electrolytes Using the Pouch Bag Method," *J. Electrochem. Soc.*, **164**, A340 (2017).
7. L. Ma et al., "A Guide to Ethylene Carbonate-Free Electrolyte Making for Li-Ion Cells," *J. Electrochem. Soc.*, **164**, A5008 (2017).
8. H. Nakai, T. Kubota, A. Kita, and A. Kawashima, "Investigation of the Solid Electrolyte Interphase Formed by Fluoroethylene Carbonate on Si Electrodes," *J. Electrochem. Soc.*, **158**, A798 (2011).
9. S. Dalavi, P. Guduru, and B. L. Lucht, "Performance Enhancing Electrolyte Additives for Lithium Ion Batteries with Silicon Anodes," *J. Electrochem. Soc.*, **159**, A642 (2012).
10. C. C. Nguyen and B. L. Lucht, "Comparative Study of Fluoroethylene Carbonate and Vinylene Carbonate for Silicon Anodes in Lithium Ion Batteries," *J. Electrochem. Soc.*, **161**, 1933 (2014).
11. K. Leung et al., "Modeling Electrochemical Decomposition of Fluoroethylene Carbonate on Silicon Anode Surfaces in Lithium Ion Batteries," *J. Electrochem. Soc.*, **161**, A213 (2013).
12. N. S. Choi et al., "Effect of fluoroethylene carbonate additive on interfacial properties of silicon thin-film electrode.," *J. Power Sources*, **161**, 1254 (2006).
13. L. J. Krause, L. D. Jensen, and J. R. Dahn, "Measurement of Parasitic Reactions in Li Ion Cells by Electrochemical Calorimetry," *J. Electrochem. Soc.*, **159**, A937 (2012).
14. L. J. Krause, L. D. Jensen, and V. L. Chevrier, "Measurement of Li-Ion Battery Electrolyte Stability by Electrochemical Calorimetry," *J. Electrochem. Soc.*, **164**, A1 (2017).
15. V. L. Chevrier et al., "Evaluating Si-Based Materials for Li-Ion Batteries in Commercially Relevant Negative Electrodes," *J. Electrochem. Soc.*, **161**, A783 (2014).